Shaking Table Response of RC Bridge Piers with Lap-Spliced Longitudinal Steels in Low Seismic Regions

Young S. Chung[1], Hong K. Hong[2], Dong W. Yang[2], and Kwang S. Lee[3]

[1] *Professor, Dept. of Civil Engineering , Chung-Ang University, Seoul, Korea Email: chung47@cau.ac.kr*
[2] *Graduate Student, Dept. of Civil Engineering , Chung-Ang University, Seoul, Korea*
[3] *PhD Candidate, Dept. of Civil Engineering , Chung-Ang University, Seoul, Korea*

ABSTRACT: The near fault ground motion (NFGM) is characterized by a single long period velocity pulse of large magnitude.(Somerville et. al 1997) Extensive research for the far fault ground motion (FFGM) have been carried out in strong seismic region, but limited research have been done for NFGM in low or moderate seismic regions because of very few records. For reinforced concrete (RC) bridge piers constructed before implementing the 1992 seismic design code in Korea, longitudinal reinforcing steels were practically lap-spliced in the plastic hinge region between column and footing. This research aims at investigating the seismic behavior of RC bridge piers with lap-spliced longitudinal steels subjected to NFGM in low or moderate seismic region. Five RC pier specimens with a diameter of 400 mm and height of 1400 mm were tested on a shake table, and two identical specimens were tested under a quasi-static load and a pseudo-dynamic load. The effects of lap-spliced longitudinal reinforcing steels are investigated. Shaking test results are compared to those by Quasi-static test and Pseudo-dynamic test. It was concluded that: a) displacement ductility was significantly decreased in RC column specimens with lap-spliced longitudinal reinforcing steels; b) bond failure in the lapped starter bars and buckling of the longitudinal steel bars initiated failure in RC specimens with and without lap-spliced longitudinal steels, respectively; c) more transverse reinforcing steels induced better displacement ductility; and d) a decrease of displacement ductility and energy dissipation was observed in the specimens on a shake table excitation in comparison with the specimens by the quasi-static and the pseudo-dynamic test.

KEYWORDS: bridges, reinforced concrete, piers, ductility, lap-splice, near fault ground motion, shake table, quasi-static, pseudo-dynamic, low seismic region.

1. INTRODUCTION

The recent earthquakes have caused extensive damage to highway bridge structures with many loss of life. The damage of bridge piers with the plastic hinge regions that experience inelastic action depends on the characteristics of earthquakes as well as column details. Failure of these structures showed a number of structural deficiencies in many bridges constructed before recent seismic design codes were in place. In particular, concrete columns with inadequate lateral reinforcement contributed to the catastrophic collapse of many bridges, and the poor detailing of the lapped starter bars in these columns compounded the problem of seismic deficiency. Plastic hinge regions with poor confinement and lap splice experienced rapid flexural strength degradation as a result of concrete cracking and splice slippage, but those with no splices and poor confinement exhibited moderate ductility with eventual degradation due to longitudinal bar buckling. In addition, current seismic design criteria for RC bridge columns, which were developed based on far-field ground motions,(Chung et. al 2003) overlook the potentially adverse effects due to near-field forward directivity pulses. This is because the majority of near-fault ground motions have been recorded only in recent earthquakes; the 1994 Northridge earthquakes, the 1995 Hyogoken Nanbu earthquakes, and the 1999 Chi-Chi earthquakes.(Phan et. al 2005) The response on structures that these motions produce is not yet well understood, and thus the effect of high velocity earthquake pulse close to active fault lines has only recently been realized to be potentially important on infrastructures. In sites located in front of the rupture direction, strong and short-duration velocity pulses associated with large ground displacement can potentially cause substantial damage.

For reinforced concrete (RC) bridge piers constructed before implementing the 1992 seismic design code in Korea, longitudinal reinforcing steels were practically lap-spliced in the plastic hinge region between column

and footing. The goal of this research aims at investigating the seismic performance of RC bridge columns with lap-spliced longitudinal reinforcing steels subjected to NFGM in low or moderate seismic region. To accomplish these goals, five RC pier specimens with a diameter of 400 mm and height of 1400 mm were tested on a shake table, and two identical specimens were tested under a quasi-static load and a pseudo-dynamic load. The effects of lap-spliced longitudinal reinforcing steels are investigated. Shaking test results are also compared to those by Quasi-static test and Pseudo-dynamic test.

2. TEST

2.1 Test specimens

The shake table has dimension of 5m x 3m and payload of 300kN. Maximum moment capacity of the table is 500kN· m and maximum displacement is ±100mm. These dimensions of the shake table limited the size of test specimens and the magnitude of near-fault ground motions. Because of the payload limitation, scaled models were designed and the axial load was introduced by pre-stressing the force at the center of the column. All specimens have a diameter (D) of 400 mm and height (H) of 1400 mm which give an aspect ratio (H/D) as 3.5.

Table 1 shows detailed dimensions of all test columns. As summarized in Table 1, test parameters were the confinement steel ratio, lap splice, and test method. Five specimens were tested on the shake table, and two identical specimens were tested under a quasi-static load and a pseudo-dynamic load. Four specimens were non-seismically designed including two specimens with lap-spliced longitudinal reinforcing steels in the plastic hinge regions. Two specimens were designed in accordance with the limited ductile design concept similar to the Euro code 8, and one specimen was constructed in conformity with the 1992 seismic design code of Korea bridge design specification.

Table 1 Specimen Design Details

<table>
<tr><th rowspan="2">Design Method</th><th rowspan="2">Specimen</th><th rowspan="2">Diameter, D
Height, H (mm)</th><th colspan="2">Longitudinal Steel</th><th colspan="2">Transverse Steel</th><th rowspan="2">Test Method</th></tr>
<tr><th>Sectional Area Ratio</th><th>Lap splice Ratio</th><th>Volumetric Confinement Steel Ratio</th><th>Space (mm)</th></tr>
<tr><td rowspan="4">Non-Seismic</td><td>RC-N-SP00-S</td><td rowspan="6">D=400
H=1,400</td><td rowspan="6">16D13
=1.61%</td><td>0%</td><td rowspan="4">0.27%</td><td rowspan="4">130/130</td><td>Shake Table</td></tr>
<tr><td>RC-N-SP50-S</td><td>50%</td><td rowspan="3">Quasi-Static</td></tr>
<tr><td>RC-N-SP00-Q</td><td rowspan="3">0%</td></tr>
<tr><td>RC-N-SP00-P</td><td>Pseudo-dynamic</td></tr>
<tr><td rowspan="2">Limit-Ductile</td><td>RC-L-SP00-S</td><td rowspan="2">0.45%</td><td rowspan="2">70/100</td><td rowspan="3">Shake Table</td></tr>
<tr><td>RC-L-SP50-S</td><td rowspan="2">50%</td></tr>
<tr><td>Seismic</td><td>RC-S-SP50-S</td><td>1.16%</td><td>30/60</td></tr>
</table>

All column specimens were longitudinally reinforced with 16D13 bars, resulting in a sectional area ratio of 1.61 percent for longitudinal reinforcing steels. The yield strength for these bars was measured as 320MPa. Transverse confining steels were provided by D6 deformed steel with an yield strength of 320MPa. As shown in Table 1, volumetric confinement steel in the plastic hinge region is in the ratio of 0.27%, 0.45%, and 1.16% for non-seismic design specimen, limited ductile design specimen, and seismic design specimen, respectively. The 28 days compressive strength of concrete was measured as 27MPa.

2.2 Test setup

The shake table at the research center of Hyundai E&C Co., Ltd was used with testing equipments for a quasi-static test and pseudo-dynamic test. While the shake table provides the input ground motions, an axial load and lateral inertial force are needed to complete the shaking test system. To assure the safety at the failure of each specimen on a shake table, the axial load and the inertial mass were separated. Sliding steel frame called as the mass rig was designed and implemented to completely support the inertial mass off of the column and the

shake table system as shown in Fig. 1. The mass rig is connected to the column head by a ball joint swivel-ended link. The effect of the mass rig on the performance of the column and the system was evaluated to provide similar characteristics to that of using mass on the top of the column. The mass rig was designed to move back and forth with little frictional resistance of less than 0.01. Post-tensioning steel tendons were used to apply an axial load of $0.1A_g f_c^{'}$ to the column.

For a quasi-static test and a pseudo-dynamic test, the test setup was conventionally designed for testing column-footing assemblages subjected to a combination of axial and lateral loadings. The constant axial load of $0.1A_g f_c^{'}$ was applied to the top of the column through post-tensioning steel tendons, and displacement-controlled lateral force cycles were simultaneously applied to the column by a 1,000 kN hydraulic actuator mounted on the retaining wall.

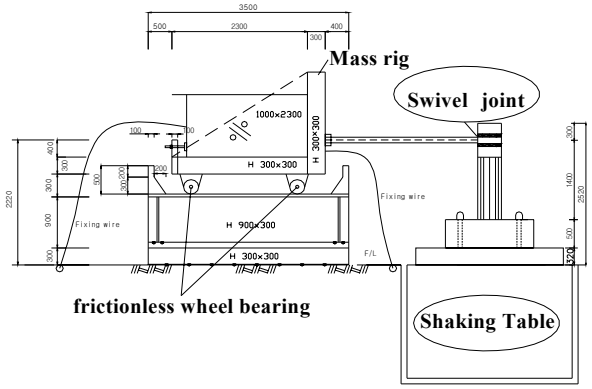

Figure 1 Test Set up

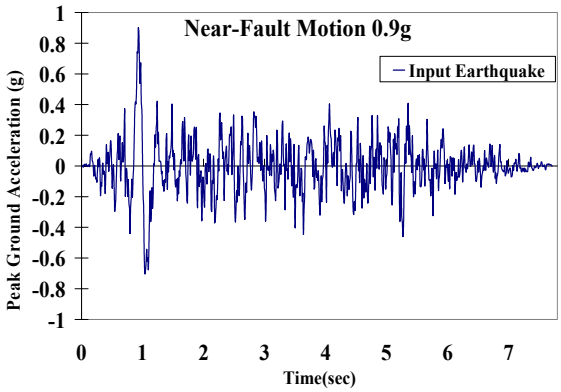

Figure 2 Input Ground Motion with a PGA of 0.9g

A quasi-static test typically consists of increasing amplitudes of displacement-controlled cycles laterally applied to a specimen until failure occurs, assessing both cumulative damage and force-displacement envelopes. A pseudo-dynamic test is similar to a quasi-static test except for inputting real earthquake motions, which are simulated by displacement-controlled cycles based on standard step-by-step linear analyses. The Newmark's explicit β algorithm was used for this research. For a shake table test, series of near fault ground motion with increasing peak ground acceleration (PGA) were selected because of being a representative typical near-fault earthquake in stable continental regions.

The near fault ground motion is characterized by a single long period velocity pulse of large magnitude. Fig. 2 shows one of input motions with a PGA of 0.9g.(Kim, J.H et. al 2006) An input motion was also examined by comparing with an acceleration data measured at the base of the specimen. Various types of instrumentations were used to observe the internal strains, displacements, accelerations, and forces during the excitation. Most instrumentation devices were located in the plastic hinge region.

3. Test Result

3.1 Load vs. Displacement Hysteretic Loop

Since all the specimens for this research were designed with a strong footing and in a flexural-shear failure mode, most of cracking damages were concentrated within the plastic hinge region of the columns. Most of the specimens failed due to the bond slippage failure of lap-spliced longitudinal steels, and failed due to the buckling of non-spliced longitudinal reinforcements. Most of the specimens developed flexural cracks in the plastic hinge area on shake table excitations, and then cover concrete spalled off.

Figs. 3 and 4 show the comparative lateral force-displacement curve during shaking table excitations. Figs. 3(b) and 4(b) show that the limited ductile specimen without lap splice developed more ductile hysteretic loops than the specimen with lap splice of 50% longitudinal reinforcing steels. Similarly, Figs. 3(a) and 4(a) show that the non-seismic specimen without lap splice developed more ductile behavior than the specimen with lap splice of 50% longitudinal reinforcing steels. In addition, Figs. 3(a), 3(b), and 3(c) showed that test specimens with more confinement steels could have greater displacement ductility. Figure 5 shows the load-

displacement curve of non-seismic specimens without lap spliced steels by the Quasi-Static and Pseudo Dynamic test. It can be known from Figs. 4(a), 5(a), and 5(b) that specimen under shaking table excitations show less ductile than the specimens by the Quasi-Static test and Pseudo Dynamic test.

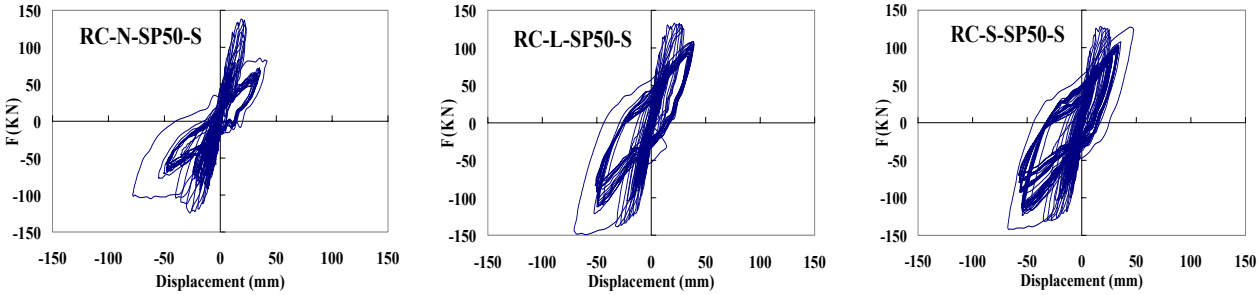

(a) RC-N-SP50-S (b) RC-L-SP50-S (c) RC-S-SP50-S

Figure 3 Force-Displacement Response for Specimens w/o Lap-Spliced Steels on a Shake Table Test

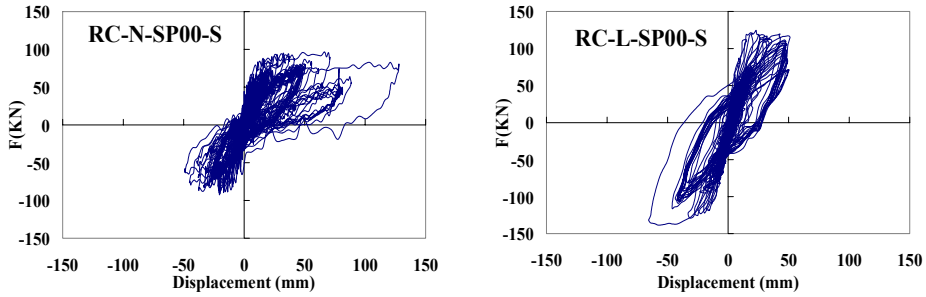

(a) RC-N-SP00-S (b) RC-L-SP00-S

Figure 4 Force-Displacement Response for Specimens w/ Non-Spliced Steels on a Shake Table Test

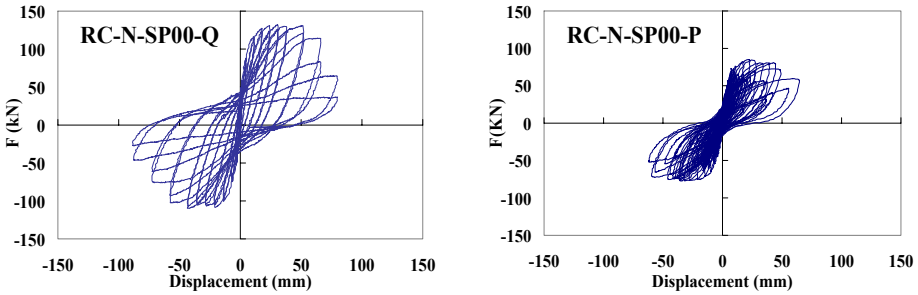

(a) RC-N-SP00-Q (b) RC-N-SP00-P

Figure 5 Force-Displacement Response for Specimens w/o Lap-Spliced Steels by the Quasi-Static and Pseudo Dynamic Test

3.2 Displacement Ductility

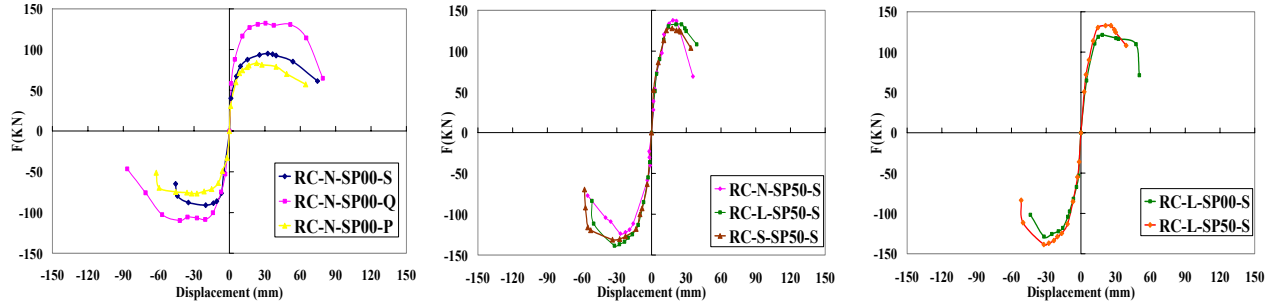

(a) Test Method (b) Design Method (c) Lap Splice

Figure 6 Envelope Curves of Lateral Force-Displacement Hysteretic Loops

Figure 6 shows the comparative force-displacement envelope curve for all test specimens in terms of test method, design method, and lap splice. The maximum lateral forces of all specimens are not much different, since the lateral confinement is effective after maximum lateral force. As shown Figure 6(a), the displacement ductility of all three specimens seemed to be approximately close because of pretty different yield displacement. However, specimen RC-N-SP00-Q shows relatively big ultimate displacement. Figure 6(b) shows that more volumetric confinement steel generally increases the displacement ductility. Figure 6(c) shows that the specimen with lap-spliced steels incurred rapid deterioration in its strength due to the bond slippage failure of the starter bars.

Table 2 Displacement ductility

Specimen	At Yield State		At Ultimate State		Displacement Ductility
	Force (KN)	Displacement (mm)	Force (KN)	Displacement (mm)	
RC-N-SP00-S	71.31 -68.24	9.39 -8.25	80.82 -77.34	57.60 -44.37	6.14 5.38
RC-N-SP50-S	103.28 -92.83	12.52 -15.39	117.05 -105.21	28.78 -39.12	2.05 2.54
RC-N-SP00-Q	99.19 -82.31	9.42 -12.12	112.41 -93.29	65.11 -61.91	6.97 5.11
RC-N-SP00-P	62.52 -57.39	8.29 -10.66	70.86 -65.04	47.66 -65.04	5.75 6.10
RC-L-SP00-S	90.99 -86.68	11.88 -11.05	103.12 -98.24	48.04 -43.55	4.04 3.94
RC-L-SP50-S	99.6 -103.9	11.13 -13.37	112.87 -117.75	36.43 -45.78	3.27 3.42
RC-S-SP50-S	95.905 -98.363	10.09 -12.81	108.69 -111.48	31.81 -55.41	3.15 4.33

In addition, the ultimate displacement was defined as the experienced maximum displacement before the fracture point when longitudinal or confinement steel exceed its fracture state, or the strength on the descending branch of the force-displacement envelope curve becomes less than $0.85V_{max}$. The displacement ductility, $\mu_\Delta = \Delta_u / \Delta_y$, was computed in Table 2.

As shown in Table 2, the displacement ductility of lap-spliced specimen RC-L-SP50-S was significantly reduced to approximate 70% of that for non-spliced specimen RC-L-SP00-S. The displacement ductility of all three specimens, RC-N-SP00-S, RC-N-SP00-P, and RC-N-SP00-Q seemed to be approximately close because of pretty different yield displacement. However, specimen RC-N-SP00-Q has relatively bigger ultimate displacement. From three specimens, RC-N-SP50-S, RC-L-SP50-S, and RC-S-SP50-S of Table 2, it is found that more volumetric confinement steel generally increases the displacement ductility.

3.3 Natural frequency and damping ratio

To achieve these dynamic characteristics of all specimens, the Fast Fourier Transform was first performed on acceleration time histories, which were measured at an accelerometer attached at the top of the specimen. Figure 7 shows three power spectrums with natural frequency of the specimen RC-N-SP50-S in terms of three PGA's. Then, damping ratios of all specimens were computed by using the Half-Power Bandwidth Methodology on the power spectrum. Table 3 shows natural frequency and damping ratio for all specimens. It was found in Table 3 that input acceleration motion with larger PGA induced a lower natural frequency and a higher damping ratio.

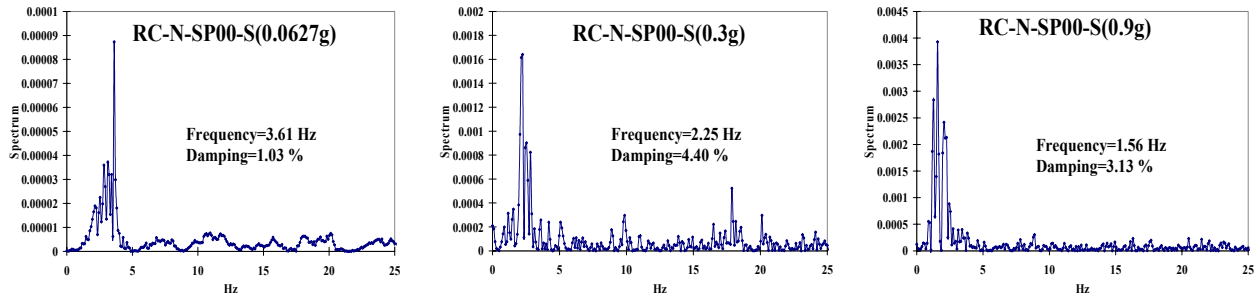

(a) PGA=0.0627g (b) PGA=0.3g (c) PGA=0.9g

Figure 7 Power Spectrum Curve of the Specimen RC-N-SP00-S in terms of a PGA

Table 3 Natural Frequency and Damping ratio

PGA	RC-N-SP00-S		RC-N-SP50-S		RC-L-SP00-S		RC-L-SP50-S		RC-S-SP50-S	
	(1)	(2)	(1)	(2)	(1)	(2)	(1)	(2)	(1)	(2)
0.0627g	3.61	1.03	3.61	1.31	3.72	1.33	3.61	1.3	3.61	1.02
0.0803g	3.61	1.05	3.61	1.42	3.72	1.33	3.61	1.38	3.61	1.15
0.11g	3.61	1.14	3.61	1.22	3.72	1.30	3.61	1.37	3.61	1.20
0.154g	2.83	3.55	3.61	2.48	3.72	1.05	3.61	1.15	3.61	1.08
0.22g	2.25	4.90	2.83	1.88	2.92	2.90	2.83	2.59	2.83	2.18
0.3g	2.25	4.40	2.54	3.33	2.21	6.68	2.54	3.84	2.44	6.73
0.4g	2.05	5.26	2.15	7.80	2.21	6.57	2.15	9.39	2.15	6.10
0.5g	2.05	3.72	2.15	6.67	2.21	6.57	2.15	6.03	2.15	5.24
0.6g	2.05	2.85	2.05	16.15	2.21	8.17	2.15	9.22	2.15	7.44
0.7g	2.05	3.40	1.56	2.97	2.11	6.73	2.15	9.17	2.15	7.72
0.8g	1.56	3.50	1.56	3.30	2.11	8.29	2.15	9.75	2.15	9.14
0.9g	1.56	3.13	2.15	7.80	2.11	7.75	2.15	9.39	2.15	7.42
*(1) = Natural Frequency, (2) = Damping Ratio										

3.4 Dissipated energy capacity

Figure 8 shows comparative curves of the cumulative energy absorption capacity of all test specimens. The amount of absorption energy in each peak ground excitation was calculated from the force-displacement hysteretic loop. As shown at 0.9g PGA of Figure 8, the non-seismic specimen RC-N-SP50-S and the limited ductile specimen RC-L-SP50-S showed a 117% and 113% higher energy absorption capacity than the seismic specimen RC-S-SP50-S, respectively. It was also known from Figure 8 that increased transverse confinement in the plastic hinge region gave bigger energy absorption capacity. Figure 8 shows that the energy absorption capacity of the non-seismic specimen, RC-N-SP00-P, by a pseudo-dynamic test was better than the identical specimen, RC-N-SP00-S, on a shake table test. Regardless of lap-spliced longitudinal reinforcing steels, the dissipated energy capacity of two specimens, RC-L-SP00-S and RC-L-SP50-S is approximately close, which would be further investigated in future.

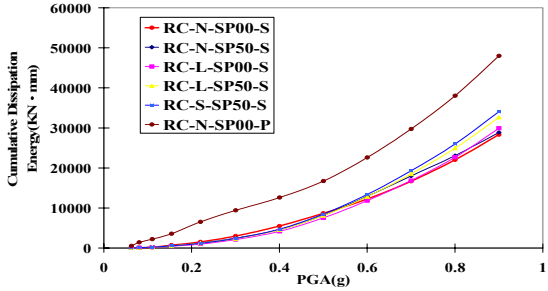

Figure 8 Accumulative dissipated energy capacity

3.5 Load vs. Strain Responses

Figure 9 shows the load vs. strain hysteretic curve of longitudinal reinforcing steels with the envelope at 0.22g for the specimen RC-N-SP00-S. Similarly, Figure 10 also shows the load vs. strain of transverse reinforcing steels with the envelope for the same specimen. All envelope curves to each PGA for every specimen can be overlapped in one figure, as shown in Figs.11 and 12 for longitudinal and transverse reinforcing steels, respectively.

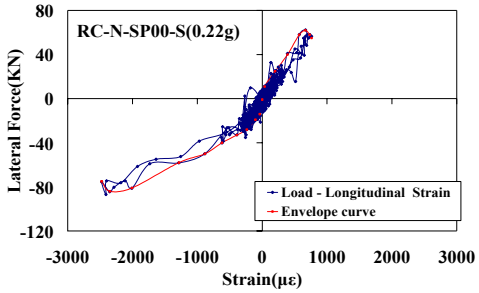

Figure 9 Load vs. Strain Curve of longitudinal steel for Specimen RC-N-SP00-S at 0.22g PGA

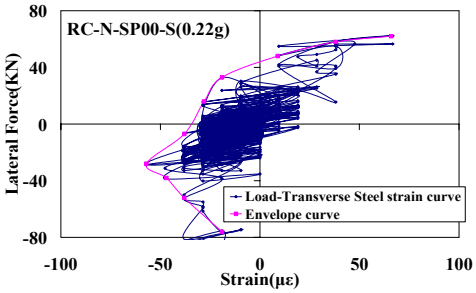

Figure 10 Load vs. Strain Curve of Transverse steel for Specimen RC-N-SP00-S at 0.22g PGA

3.5.1 Envelope on the Load vs. Strain Responses of Longitudinal Steels

Figure 11 shows all envelopes on the load vs. strain hysteretic curve of longitudinal reinforcing steels when they were initially fractured for the specimens RC-N-SP00-S and RC-L-SP00-S, respectively. As shown in Figs. 11(a) and (b), longitudinal steel of specimens RC-N-SP00-S and RC-L-SP00-S was initially fractured at the PGA of 0.4g and 0.5g, respectively. This result implies that more confinement steels gives bigger ultimate strain of longitudinal steels to be fractured at bigger lateral load.

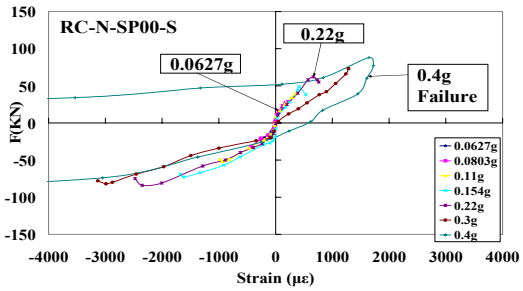

(a) RC-N-SP00-S

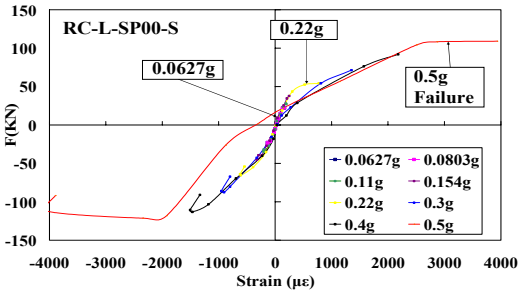

(b) RC-L-SP00-S

Figure 11 Envelope on the Load vs. Strain Curve Longitudinal steels

3.5.2Envelope on the Load vs. Strain Responses of Transverse Steels

Figs. 12(a) and 12(b) show all envelopes on the load vs. strain hysteretic curve of transverse reinforcing steels for the specimens RC-N-SP00-S and RC-L-SP00-S, respectively. As shown in Figure 12, transverse steel of both specimens was not fractured until the specimen failed. It was found from Figure 12 that when a PGA increased, the origin and the slope of envelope curves gradually moved to the right of the x axis and became flat, respectively.

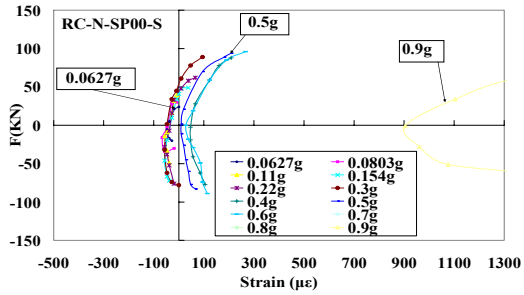

(a) RC-N-SP00-S

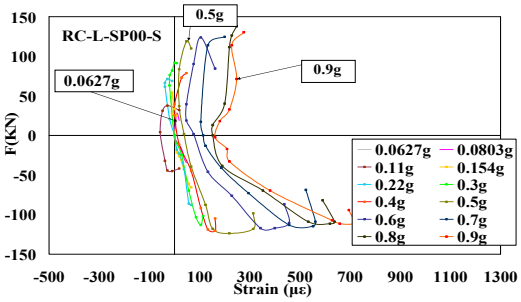

(b) RC-L-SP00-S

Figure 12 Envelope on the Load vs. Strain Curve Transverse steels

4. Conclusions

The shaking table test for RC columns was performed to investigate their seismic behavior, together with a quasi-static test and a pseudo-dynamic test. It was concluded that:

1) displacement ductility was significantly decreased in RC column specimens with lap-spliced longitudinal reinforcing steels;

2) bond failure in the lapped starter bars and buckling of the longitudinal steel bars initiated failure in RC specimens with and without lap-spliced longitudinal steels, respectively;

3) more transverse reinforcing steels induced better displacement ductility;

4) a decrease of displacement ductility and energy dissipation was observed in the specimens on a shake table excitation in comparison with the specimens by the quasi-static and the pseudo-dynamic test; and

5) more confinement steels gave bigger ultimate strain of longitudinal steels to be initially fractured at bigger PGA.

ACKNOWLEDGEMENT

The authors gratefully acknowledge the support of the Infra-Structures Assessment Research Center (ISARC-04C02-02) funded by the Korea Ministry of Construction and Transportation (MOCT).

REFERENCES

AASHTO. (2004). LRFD Bridge Design Specification, American Association of State Highway and Transportation Officials, USA.

ACI 318R-05. (2005). Building code requirements for structural concrete ACI 318-05 and commentary, American Concrete Institute. USA.

AISC-LRFD. (1999). Load and Resistance Factor Design Specification for Structural Steel Buildings, American Institution of Steel Construction, USA.

Somerville, P.G., Smith, N.F., and Graves, R.W.(1997). Modification of Empirical Strong Ground Motion Attenuation Relations to Include the Amplitude and Duration Effects of Rupture Directivity. *Seismological Research Letters*, **Vol. 68, No. 1**.

Chung, Y.S., Park, C.K., Park, J.Y. (2003). Seismic Performance Evaluation of RC Bridge Piers with Limited Ductility by the Pseudo-Dynamic Test, *A Journal of the Korea Concrete Institute*, **Vol. 15, No. 5**, pp. 705-714.

Chung, Y.S., Park, C.K., Meyer. (2008). Residual Seismic Performance of Reinforced Concrete Bridge Piers after Moderate Earthquakes, *A Journal of the American Concrete Institute*, **Vol. 105, No. 1**, pp. 87-95.

Vu T.Phan, M.Saiid Saiidi, J. Anderson.(2005). Near Fault Ground Motion Effects on Reinforced Concrete Bridge Columns. *Center of Civil Engineering Earthquake Research, Department of Civil and Environmental Engineering*, University of Nevada, Reno, Report No. CCEER-05-7.

Kim, J.H. and Kim, J.K. (2006). Modeling of near fault ground motion due to moderate magnitude earthquakes in stable continental regions, *Journal of the earthquake engineering society of Korea*, **Vol. 10, No. 3**, pp. 101-111.